Chapter 4

Evolution of shock waves in dusty non-ideal gas flow with magnetic field *

4.1 Introduction

This chapter deals with the study of propagation of shock waves in two dimensional steady supersonic magnetogasdynamics flow of non-ideal dusty gas using wavefront analysis method. The study of non-linear PDEs is a significant research area in applied mathematics, theoretical physics, and engineering due to the rapid advancement of science and technology. It plays a vital role in numerous branches e.g., astrophysics, cosmology, space research, aerospace science, combustion theory, etc. It's salient feature is that their solutions encounter discontinuities such as shock

* "The contents of this chapter have been published in ***Zeitschrift für Naturforschung A (De Gruyter), 2024.***"

waves. Shock wave study has gained more attention due to it's application in various domains, including aerodynamics, astrophysics, plasma physics, solid-state physics, optical fibers, geophysics, biomechanics, and nuclear science. Shock wave arise due to sudden changes in the flow variables. In recent years, it has a wide range of applications due to energetic events and they become usual in the interstellar medium. It also has various applications in medicine. Due to shock waves, solid foods have a better chance of bacterial survival than liquid or foamy ones. The evolution of shocks is well understood by flattening or steepening of ordinary waves, e.g., neutron stars, black holes, heavy explosions generating supersonic explosions, and ocean waves breaking on the shore. Zeidan [138] investigated the evolutionary behavior of polyatomic gases using the Lie symmetry method. Shen[139] studied a zero-pressure one-dimensional gas dynamics system and obtained a unique β- solution, which is compared with known results. Tomar et al.[72] discussed existence of shock and its location using perturbation series technique.

Sahu[140] showed the influence of the magnetic and gravitational field on the cylindrically symmetric motion of inviscid non-ideal gas using the method of self similarity where numerical computations are done by Runge-Kutta method of order four. Yadav et al.[141] obtained approximate solution of cylindrical shocks in rotational axisymmetric ideal gas using the Sakurai's technique in terms of power series. Chaturvedi et al.[103] investigated the growth and decay behaviour of non-ideal relaxing gas using the characteristic method. Yadav et al.[142] analyzed the evolution of cylindrical shocks in adiabatic flow of non-ideal gas and obtained self-similar solution using Lie group technique. Using progressive wave approach Nath, Gupta and Singh[40] analyzed the propagation of disturbances in dusty gas and acquired the condition of shock formation.

The impact of magnetic field on the evolution of shocks comprises a significant problem for the authors in various fields of science, specifically in the study of coronal

heating problems, which can be linked to the topic "why the temperature of the Sun's corona is significantly greater than that of its surface". Bira and Sekhar[122] investigated the impact of the magnetic field on the radially symmetric motion of a perfectly conducting non-ideal gas. Zeidan et al.[143] analyzed one dimensional motion of magnetogasdynamics equation explicitly for reflected and transmitted wave. Canupp[144] studied essential features of magnetogasdynamics shock structure, demonstrating the non-monotonic nature of entropy and explaining how a large magnetic field modified the shock structure. Giacalone[145] examined the influence of density on the magnetic shock waves via solving numerical simulations of two-dimensional magnetohydrodynamic equations. Singh[146] studied the flow pattern driven by a piston behind an exponential shock under the effect of magnetic field using self-similar method.

Shock waves propagating in gases containing solid or liquid particles have been the subject of extensive scientific and technical study over the past three decades. This interest originates from the fact that in many engineering problems, the presence of dust particles has a significant impact on the shock wave discontinuous waves, such as flow in jet engines with turbine blades, dusty terrain with nuclear explosions, formation of stars, volcanic explosions, underground explosions, the polluted crystals formation, and many more. Many research papers are concerned with the above-stated problems (see [110], [147], [148], [94]). With the help of similarity transformation method, Chauhan[149] studied one-dimensional unsteady cylindrical flow and showed the effect of various parameters. Nath and Devi[150] investigated the evolution of shocks in self-gravitating medium with dust particles, for unsteady adiabatic and isothermal flow. Gupta et al.[147] derived an asymptotic solution of one-dimensional compressible unsteady planar and non-planar flows in dusty gas using weakly non-linear geometrical acoustics. In a gas containing dust particles, Amin et al.[151] used the power series expansion method to solve the problem of

strong plane and cylindrical shocks. Therefore, shock wave's study in a gas containing small dust particles with magnetic field has great importance. Sharma et al.[152] studied the propagation of waves in a flow with axial magnetic field and dust particles and investigated the behavior of flow variables using singular surface theory and compatibility equation. Srivastava et al.[113] investigated propagation of weak discontinuities under the impact of magnetic field in non-ideal dusty flow using method of characteristics. The similarity solutions for cylindrical shock wave in a mixture of perfect gas with solid particles have been obtained in Vishwakarma, Nath, and Srivastava[153]. Yadav[141] analyzed the impact of magnetic field on the evolution of dusty shocks with isothermal flow using the power series method. Nath[154] derived closed-form solution of blast wave for isothermal and adiabatic flow under the influence of magnetic field and dust particles. Sahu[155] examined the propagation of cylindrical shocks in the presence of magnetic field with dust particles and obtained similarity solutions. [118] studied the propagation of shocks in mixture of small-sized dust particles with magnetic field and discussed the impact of various parameters on the formation of shocks.

In this chapter, we investigate a system of non-linear PDEs that models the dusty non-ideal gas flow under the influence of magnetic field. The proposed governing equations are very complex and require extra effort to find it's solution. It seems worthwhile to give a broader discussion of these effects for general wave propagation problems and investigate all the possible inferences. Aim of the present chapter is to study the effect of interaction of dust particles and magnetic field in non-ideal gas on the evolution of shock wave. The wavefront analysis method is applied to assess the various aspects of non-linear wave propagation. The content of the chapter is organized in the following manner: Sec. 4.2 contains mathematical model describing two-dimensional steady supersonic flows of non-ideal dusty gas with magnetic field

and its characteristic formulation. By introducing new curvilinear coordinates, the transport equations for the discontinuity wave are derived in Sec. 4.3. The next section discusses shock wave propagation using the solution of transport equation. In Sec. 4.5, we have analyzed the findings of this study for plane beak and axisymmetric flow, and Sec. 4.6 concludes this work.

4.2 Mathematical Model of the problem

The mathematical model for the 2-D steady supersonic dusty non-ideal flow of gas under the influence of magnetic field may be written as (See Vishwakarma et al. ([156, 157]), Pai et al. [53])

$$\begin{aligned} u\rho_x + v\rho_y + \rho(u_x + v_y) &= -\frac{\rho n v}{y}, \\ \rho u u_x + \rho v u_y + p_x + h_x &= 0, \\ \rho u v_x + \rho v v_y + p_y + h_y &= 0, \\ u h_x + v h_y + 2h(u_x + v_y) &= -\frac{2hnv}{y}, \\ u p_x + v p_y - C^2(u\rho_x + v\rho_y) &= 0, \end{aligned} \tag{4.1}$$

where u, v, ρ, p denote velocity components along the x and y axis, density and pressure, respectively. The quantity $h = \frac{\mu H^2}{2}$, indicates magnetic pressure where H and μ specifies transverse magnetic field and magnetic permeability, respectively. $n = 0, 1$ corresponds to plane beak and axisymmetric case, respectively. Here, C represents the speed of sound in non ideal dusty gas under the impact of magnetic field, given by

$$C^2 = \frac{(\Gamma - \omega_2\rho^2)p}{(1 - \omega_1\rho + \omega_2\rho^2)\rho},$$

where $\omega_1 = \phi + \overline{b}$ and $\omega_2 = \phi\overline{b}$; $\overline{b}$ is non-ideal parameter. $\Gamma = \frac{\gamma(1+\mu\kappa)}{(1+\lambda\kappa\gamma)}$, indicates *Grüneisen* coffecient with $\mu = k_p/(1-k_p)$, $\gamma = c_p/c_v$, $\kappa = c_{sp}/c_p$. The quantity c_{sp} denotes specific heat of dust particles, c_p and c_v denote the specific heat of the gas at constant pressure and constant volume, respectively. The volume fraction Z is given by $Z = V_{sp}/V_g$ where V_{sp} and V_g denote volume of the dust particles and total volume of mixture, repectively (Chadha and Jena[158]). k_p denotes mass fraction of the solid particles, given by $k_p = m_{sp}/m_g$, where m_{sp} is the mass of the solid particles, m_g is total mass of the mixture. Z and k_p are correlated by $Z = \phi\rho$, $\phi = k_p/\rho_{sp}$, where ρ_{sp} is the specific density of the dust particles.

Based on values of the quantities ϕ and $\overline{b}$, we have the following cases.

Case 1: When $\phi = 0$ and $\overline{b} \neq 0$, then Γ becomes γ, $C^2 = \frac{\gamma p}{(1-b\rho)\rho}$, i.e. the flow becomes van der Waals gas flow in a dust free medium.

Case 2: When $\phi = 0$ and $\overline{b} = 0$, then Γ becomes γ, $C^2 = \frac{\gamma p}{\rho}$, and the mixture becomes ideal in the absence of dust particles.

Case 3: When $\phi \neq 0$ and $\overline{b} = 0$, in this case $\Gamma \neq 0$, $C^2 = \frac{\Gamma p}{(1-Z)\rho}$, and the flow becomes ideal gas flow with dust particles.

Case 4: When $\phi \neq 0$ and $\overline{b} \neq 0$, in this case $\Gamma \neq 0$, $C^2 = \frac{(\Gamma-\omega_2\rho^2)p}{(1-\omega_1\rho+\omega_2\rho^2)\rho}$, and the flow becomes non-ideal gas flow with dust particles.

The equation of state is written as (Srivastava et al. [97])

$$p = \frac{(1-k_p)}{(1-Z)(1-\overline{b}\rho)}\rho RT, \tag{4.2}$$

where R and T indicates the Universal gas constant and temperature of the gas, respectively.

We can write the system (4.1) as follows

$$Q_x + R(Q)Q_y + S = 0. \tag{4.3}$$

where column vectors Q, S and the matrix R is given by

$$Q = \begin{pmatrix} \rho \\ u \\ v \\ h \\ p \end{pmatrix}, \qquad S = \frac{1}{(u^2 - d^2)} \begin{pmatrix} \frac{\rho n v u}{y} \\ -\frac{n v d^2}{y} \\ 0 \\ \frac{\rho e^2 n v u}{y} \\ \frac{\rho n v u C^2}{y} \end{pmatrix},$$

$$\text{and} \quad R = \frac{1}{(u^2 - d^2)} \begin{pmatrix} \frac{v\left(u^2-d^2\right)}{u} & -\rho v & \rho v & \frac{v}{u} & \frac{v}{u} \\ 0 & uv & -d^2 & -\frac{v}{\rho} & -\frac{v}{\rho} \\ 0 & 0 & \frac{v\left(u^2-d^2\right)}{u} & \frac{\left(u^2-d^2\right)}{\rho u} & \frac{\left(u^2-d^2\right)}{\rho u} \\ 0 & -\rho e^2 v & \rho e^2 u & \frac{v\left(u^2-C^2\right)}{u} & -\frac{v e^2}{u} \\ 0 & -\rho C^2 v & \rho C^2 u & \frac{v C^2}{u} & \frac{v\left(u^2-e^2\right)}{u} \end{pmatrix}. \tag{4.4}$$

The eigenvalues and left eigenvectors of matrix $R(Q)$ are denoted by $\lambda^{(i)}$ and $L^{(i)}$, respectively, for $1 \leq i \leq 5$, then we have

$$\lambda^{(1,2,3)} = \frac{v}{u}, \qquad \lambda^{(4,5)} = \frac{uv \pm d^2 \left(\frac{M^2}{\epsilon} - 1\right)^{1/2}}{(u^2 - d^2)}, \tag{4.5}$$

and its corresponding left eigenvectors are

$$J^{(1)} = \begin{pmatrix} 1 & 0 & 0 & 0 & -\frac{1}{C^2} \end{pmatrix}, \quad J^{(2)} = \begin{pmatrix} 0 & 1 & \frac{v}{u} & 0 & \frac{\epsilon}{\rho u} \end{pmatrix}, \quad J^{(3)} = \begin{pmatrix} 0 & 0 & 0 & 1 & 1-\epsilon \end{pmatrix},$$
$$J^{(4)} = \begin{pmatrix} 0 & 1 & -\frac{u}{v} & 0 & -\frac{\epsilon}{\rho v}\left(\frac{M^2}{\epsilon} - 1\right)^{1/2} \end{pmatrix},$$
$$J^{(5)} = \begin{pmatrix} 0 & 1 & -\frac{u}{v} & 0 & \frac{\epsilon}{\rho v}\left(\frac{M^2}{\epsilon} - 1\right)^{1/2} \end{pmatrix}. \tag{4.6}$$

Here, M is given by $M = \frac{q}{C}$, is known as upstream flow Mach number, with $q = \sqrt{u^2 + v^2}$, and the quantity $d = (C^2 + e^2)^{1/2}$ is magneto-sonic speed with $e = \sqrt{2h/\rho}$. The quantities e and ϵ are Alfvén speed and Alfvén number with

$\epsilon = 1 + \frac{e^2}{C^2}$.

From (4.5),(4.6) it is observed that the system (4.3) exhibits five real eigenvalues, indicative of supersonic flow. Correspondingly, it possesses a set of five linearly independent eigenvectors, denoted by $J^{(i)}$ for $i = 1, 2, 3, 4, 5$. Three families of characteristics i.e. $\lambda^{(1,2,3)}$ are along streamline, the remaining two $\lambda^{(4,5)}$ represent waves propagating in opposite direction along which discontinuity propagates.

4.3 Transport equation for shock wave

The main objective of the study is to analyze the evolutionary processes of the discontinuities. We are focusing to derive transport equation for jump discontinuity in Q as they move along the wavefront with $\sigma = 0$ which governs the growth and decay process of discontinuities. As in Singh et al. [56], we introduce new curvilinear coordinates σ, y' which are defined by (Jeffrey [5])

$$\sigma_x + \lambda^{(4)}\sigma_y = 0, \quad \sigma(x, y_0) = x - x_0, \quad y = y'. \tag{4.7}$$

Let $\lambda^{(4)}$ (or $\lambda^{(5)}$) describes the intial wavefront as $\sigma = 0$. Initially $\sigma = 0$ passes through (x_0, y_0), and the medium after $\sigma = 0$ is supposed to have uniform temperature $T_0 = T_b$ and uniform velocity u_0 along the x-axis with $v_0 = 0$; here suffix-0 denotes the region ahead of $\sigma = 0$. σ has required coordinate property that σ is negative (positive) behind (ahead) the wavefront $\sigma = 0$. In terms of these new coordinates with $x_\sigma = \frac{1}{\sigma_x}$ as the Jacobian of the transformation (Schmitt [159]).

System (4.3) can be defined in terms of new coordinates using Equation (4.7) after

premultiplying by $J^{(i)}$ as follows:

$$(\lambda^{(4)} - \lambda^{(i)})J^{(i)}Q_\sigma + \lambda^{(i)}\lambda^{(4)}x_\sigma J^{(i)}Q_{y'} + \lambda^{(4)}x_\sigma J^{(i)}S = 0, \tag{4.8}$$

Q and $Q_{y'}$ are continuous across the wavefront $\sigma = 0$ and have subscripts-0 values, whereas Q_σ and x_σ are discontinuous. The evaluation of (4.8) at the back side of $\sigma = 0$ for $i = 1, 2, 3, 5$, yields

$$\rho_\sigma = \frac{1}{C_0^2}p_\sigma, \tag{4.9}$$

$$u_\sigma = -\frac{\epsilon_0}{\rho_0 u_0}p_\sigma, \tag{4.10}$$

$$h_\sigma = (\epsilon_0 - 1)\, p_\sigma, \tag{4.11}$$

$$v_\sigma = \frac{\epsilon}{\rho_0 u_0}\left(\frac{M_0^2}{\epsilon_0} - 1\right)^{1/2} p_\sigma. \tag{4.12}$$

Taking $i = 4$ in (4.8), and differentiating the obtained results w.r.t. σ, then evaluating it at the rear of wavefront $\sigma = 0$, we get

$$d_0\epsilon_0\left(\frac{M_0^2}{\epsilon_0} - 1\right)^{1/2} p_{\sigma y'} + d_0 u_0 \rho_0 v_{\sigma y'} + \frac{\rho_0 n u_0 C_0}{y'}(\epsilon_0)^{1/2} v_\sigma = 0. \tag{4.13}$$

Using (4.12) in (4.13), we obtain

$$p_{\sigma y'} + \frac{n}{2y'\epsilon_0}p_\sigma = 0. \tag{4.14}$$

Along $\sigma = constant$, we get

$$x_{y'} = \frac{u^2 - d^2}{uv + d^2\left(M_0^2/\epsilon_0 - 1\right)^{1/2}}. \tag{4.15}$$

Equations (4.14) and (4.15) are the desired transport equations, which we have been

seeking.

Differentiate (4.15) w.r.t. σ and then evaluating at the rear of $\sigma = 0$ and using equation (4.14) we get,

$$x_{\sigma y'} = \frac{-M_0^2\big((\Gamma + w_1\rho_0 - 3w_2\rho^2) + \epsilon_0(1 - w_1\rho_0 + w_2\rho^2)\big)p_\sigma}{2\epsilon_0\rho_0 d^2\left(M_0^2/\epsilon_0 - 1\right)^{1/2}(1 - w_1\rho_0 + w_2\rho_0^2)}. \tag{4.16}$$

On integrating equation (4.14) with respect to y', we get

$$p_\sigma = \left(\frac{y_0}{y'}\right)^{\frac{n}{2\epsilon}} p_{\sigma_0}, \tag{4.17}$$

where $p_{\sigma_0} = \lim_{y' \to\ y_0} p_\sigma$, along $\sigma = 0$.

4.4 Propagation of shock wave

Integrating equation (4.16) with respect to y' we have

$$x_\sigma = 1 - \frac{M_0^2\big((\Gamma + w_1\rho_0 - 3w_2\rho^2) + \epsilon_0(1 - w_1\rho_0 + w_2\rho^2)\big)p_\sigma}{2\epsilon_0\rho_0 d_0^2\left(\frac{M_0^2}{\epsilon_0} - 1\right)^{1/2}(1 - w_1\rho_0 + w_2\rho_0^2)}\,(y_0)^{n/2\epsilon_0}\,p_{\sigma_0}\int_{y_0}^{y} r^{(-n/2\epsilon_0)}dr. \tag{4.18}$$

Using equation (4.7), the condition (Schmitt [159]) $x_{\sigma_0} = x_\sigma\,|_{\sigma=0^-} = x_\sigma\,|_{\sigma=0^+} = 1$, is obtained. Assuming $y = \tilde{Y}(x)$, the equation of body contour with tangent at the leading edge that is parallel to the velocity of the stream line, we get $dy/dx = v/u$, differentiating it w.r.t. σ and evaluating it at the rear of $\sigma = 0$, gives

$$v_{\sigma_0} = u_0\tilde{Y}_0'', \tag{4.19}$$

where $\tilde{Y}_0''$ is the curvature of the body at the tip.

Using (4.12) and (4.19) in (4.18), we get

$$x_\sigma = 1+\frac{2\epsilon_0\left(1-\epsilon_0\right)-M_0^2\left(\gamma+\epsilon_0+\bar{b}\left(1-\epsilon_0\right)\right)}{2\epsilon_0\left(M_0^2\left(1-\bar{b}\right)-\epsilon_0\right)}\left(y_0\right)^{n/2\epsilon_0} M_0^2\left(1-\bar{b}\right)\tilde{Y}_0''\int_{y_0}^{y} r^{(-n/2\epsilon_0)}dr. \tag{4.20}$$

If x_σ converges to zero for some $y = y_r$, then nearby characteristics of the family $\sigma = constant$ will intersect the wavefront $\sigma = 0$ and strong discontinuity will emerge in the solution vector Q which is called as a shock wave. With the assumption Q_σ is finite at $y = y_r$ as $x_\sigma = 0$ then at the back of $\sigma = 0$, $Q_x = \frac{Q_\sigma}{x_\sigma}$ becomes unbounded. This phenomenon is called as wavefront steepening. The following section provides a brief discussion about the results obtained in (4.20).

4.5 Results and discussion

Now, we deal with supersonic flow for planar($n = 0$) and axisymmetric($n = 1$) flow. The described phenomenon is sketched in Fig.4.1

4.5.1 Plane beak Case $(n = 0)$

For plane beak, putting $n = 0$ in (4.20) with body contour $y = \tilde{Y}_a(x)$ (say). Initially from sharp edge of the contour, disturbance is propagated with a small initial tangent. For this case (4.20) becomes

$$x_\sigma = 1 - \frac{\tilde{Y}_a''(0)\left(y-y_0\right)}{\chi}, \tag{4.21}$$

where

$$\chi = 2\epsilon^2(M_0^2-\epsilon_0)(1-w_1\rho_0+w_2\rho_0^2)\left(M_0^4\left(\Gamma + w_1\rho_0 - 3w_2\rho_0^2 + \epsilon_0(1 - w_1\rho_0 + w_2\rho_0^2)\right)\right)^{-1}.$$

When body contour bends, the radius of curvature at the tip is $\tilde{Y}_a''(0)$ and $\chi > 0$. As charateristics initiates to combine, the shock will form when x_σ vanishes. When body shape has a compressive corner at $x = 0$, from (4.21) we observe, when $\tilde{Y}_a''(0) > 0$ with $\tilde{Y}_a''(0) > \chi$ for $y_0 < y$ then only Jacobian will vanish on front side of wavefront. While for $\tilde{Y}_a''(0) \leq \chi$, there is no formation of shock as x_σ remains positive for finite $y_0 < y$. From this, we can say χ denotes the critical level and when at the tip of the body, $\chi > \tilde{Y}_a''(0)$, then shock is formed at some finite distance away from the body.

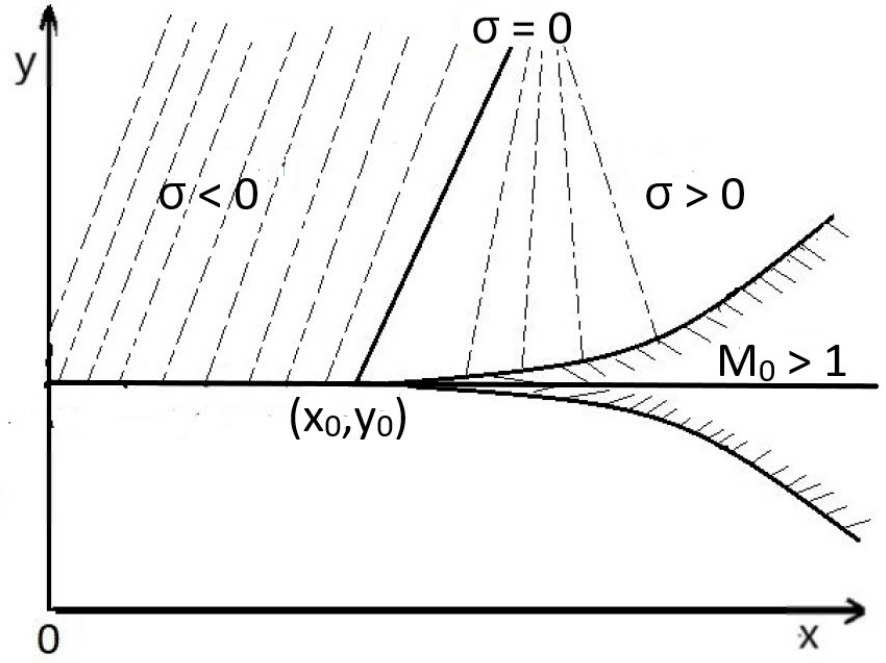

FIGURE 4.1: Convergence of the characteristics for planar and axisymmetric supersonic flow.

Now at $\sigma = 0$, v_x and v_σ are associated by relation $v_x = v_\sigma/x_\sigma$; so it makes no

difference if we look an expression for v_σ or v_x at the wavehead. We choose to work in form of v_x since it has more physical interpetations. From (4.21), (4.16) and (4.11) we have

$$v_x = \frac{d_0 M_0 \tilde{Y}_a''(0)}{\epsilon_0^{1/2}\left(1 - \frac{\tilde{Y}_a''(0)(y-y_0)}{\chi}\right)}. \tag{4.22}$$

(4.22) provides a criterion for wave to steepen or flatten.

It is clear from (4.22) that when $\tilde{Y}_a''(0)$ is positive with condition $|\tilde{Y}_a''(0)| > \chi$ then there exist a finite length y_r and wave ends into shock. The corresponding equation of shock formation distance is

$$y_r = y_0 + \frac{\chi}{\tilde{Y}_a''(0)}. \tag{4.23}$$

At $y = y_r$, denominator of (4.22) vanishes and its numerator becomes finite or we can say velocity gradient becomes unbounded at the front of wave which indicates the steepening of wave into shock wave. On the contrary, the wave is still compressive for $\tilde{Y}_a''(0) \geq \chi$ and there is no formation of shock at $\sigma = 0$. v_x either decays along the front of wave or remains stationary in accordance with $\tilde{Y}_a''(0) < \chi$ or $\tilde{Y}_a''(0) = \chi$, respectively.

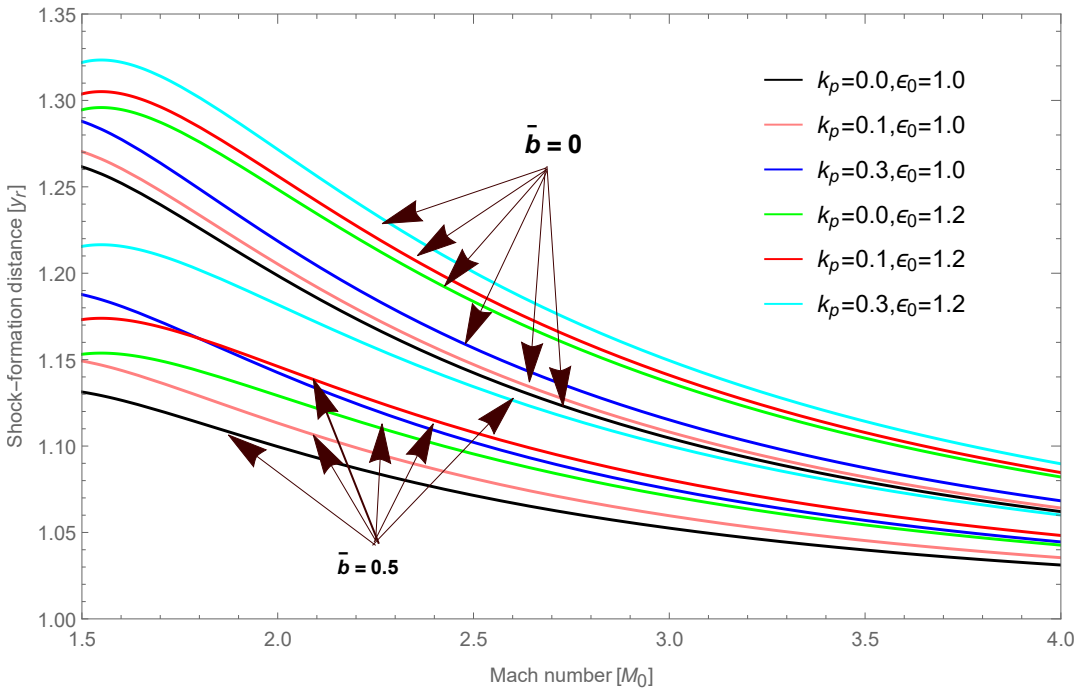

FIGURE 4.2: Influence of dust particles and magnetic field in non-ideal gas on y_r with $\gamma = 1.67$, $Z = 0.01$, $\beta = 0.8$.

The solution curves presented in Fig.5.1 shows the effect of dust particles and magnetic field for both ideal and non-ideal cases. In the presences of magnetic field, with an increase in the parameter of dust particles k_p from 0.0 to 0.3, the shock formation distance y_r increases which indicates that there is delay in shock formation. Also, an increase in magnetic field causes to deccelerate the growth of shock wave propagation. For ideal gases, there is minute delay in shock formation with increase in dust particles and magnetic field but in case of non-idael gas, the delay process accelerates and it keeps on increasing, as the presences of dust particles and magnetic field increases. More specifically we can say shock forms early in case of non-ideal gas as values attained by y_r are lesser for this case. Further, the effect of magnetic field in the presence of dust particles in non-ideal gas is to increase the shock formation distance. Also, we notice that as the Mach number increases, the shock formation distance decreases, resulting in an early shock formation.

4.5.2 Axisymmetric Case $(n = 1)$

In this case we consider a ring shaped body $y = \tilde{Y}_s(x)$ with sharp edged entry which releases the initial disturbance that spreads both within and outward along characteristic lines. Both phenomena are decribed by (4.20). For $y_0 < y$, similar phenomenon is observed as in case of plane flow. Now putting $n = 1$ into (4.20), we get

$$x_\sigma = 1 - B_0 \tilde{Y}_s''(0) \left(y^{\left(\frac{2\epsilon_0 - 1}{2\epsilon_0}\right)} - y_0^{\left(\frac{2\epsilon_0 - 1}{2\epsilon_0}\right)} \right), \tag{4.24}$$

where

$$B_0 = \frac{M_0^4 \left(\Gamma + w_1\rho_0 - 3w_2\rho_0^2 + \epsilon_0 \left(1 - w_1\rho_0 + w_2\rho_0^2\right)\right)}{\epsilon_0 \left(M_0^2 - \epsilon_0\right)\left(1 - w_1\rho_0 + w_2\rho_0^2\right)\left(2\epsilon_0 - 1\right)} y_0^{1/2\epsilon_0}. \tag{4.25}$$

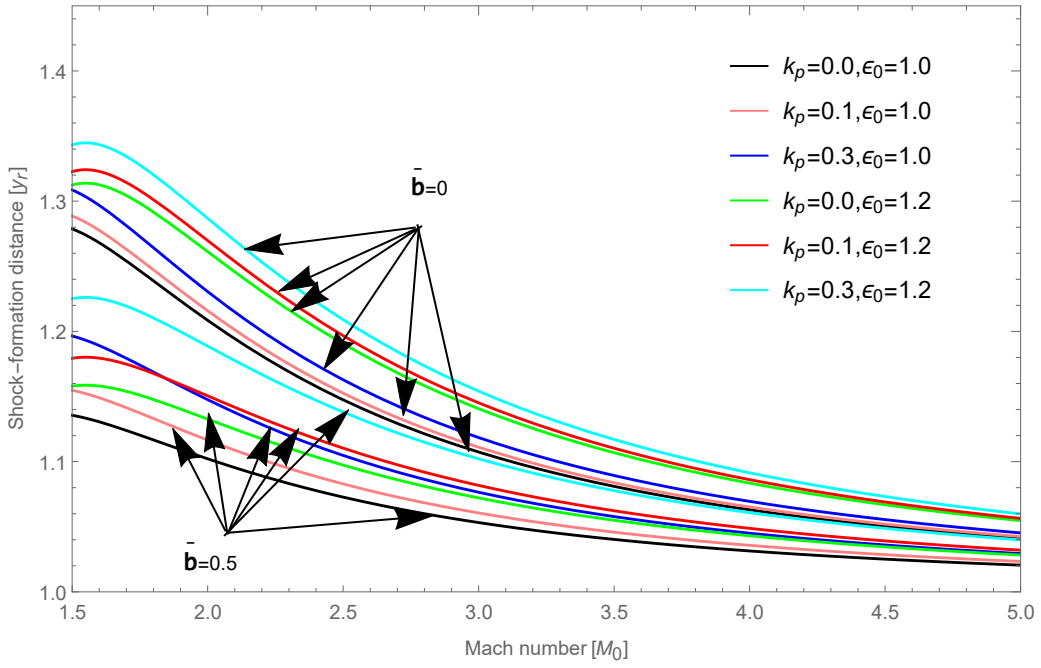

FIGURE 4.3: Influence of dust particles and magnetic field in non-ideal gas on y_r with $\gamma = 1.67$, $Z = 0.01$, $\beta = 0.8$.

From (4.24), we analyse that for $y_0 < y$, the expression enclosed in bracket is positive and can't exceed one. So x_σ tends to zero which results in occurrence of shock,

provided $\tilde{Y}_s''(0) > 0$ and $\tilde{Y}_s''(0) > B_0^{-1}$. If $\tilde{Y}_s''(0) \leq B_0^{-1}$, $x_\sigma > 0$, there is no formation of shock on the leading wavefront. Thus, we can say that the shock will form when $\tilde{Y}_s''(0) > B_0^{-1}$, then at $y = y_r$, when the first shock is formed, is given by

$$y_r = \left(y_0^\beta + \frac{1}{B_0 \tilde{Y}_s''(0)} \right)^{1/\beta}, \tag{4.26}$$

where $\beta = 1 - 0.5\epsilon_0^{-1}$. Fig. 5.4 depicts the influence of dust particles, magnetic field for both ideal and non-ideal cases. The nature of solution curves shows slight variation from plane beak case. As the presence of dust particles increases with increase in magnetic field, there is decrease in the growth of shock propagation. Also shock formation distances increases. It is clear that shock formation distance increases in both ideal and non-ideal gas but there is an early shock formation in non-ideal case as compared to idael gas. Clearly, with higher values of magnetic field parameter in the presence of dust particles, growth rate of propagaton is delayed. There is a rise in shock formation distance i.e there is delay in formation of shock. Also, we observed that with rise in Mach number causes the shock formation distance to decrease, indicating early shock formation.

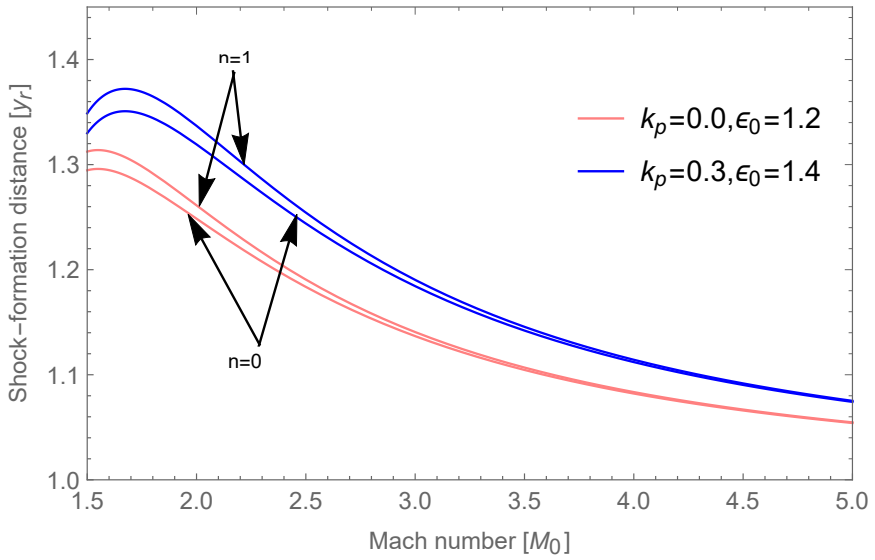

FIGURE 4.4: Comparative study of geometry of ideal($\bar{b} = 0$) dusty magneto-gasdynamics for $\gamma = 1.67$, $Z = 0.01$, $\beta = 0.8$, $\tilde{Y}_s''(0) = 0.7$.

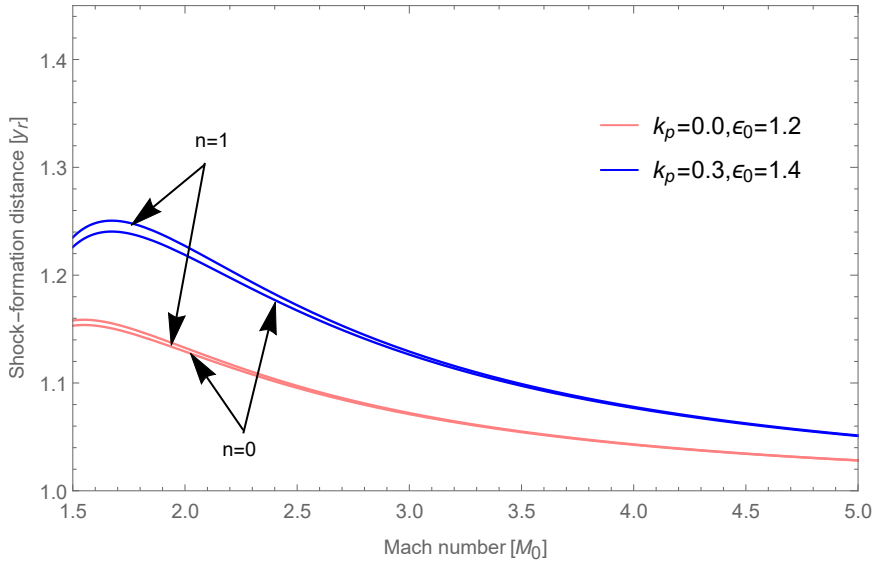

FIGURE 4.5: Comparative study of geometry of non-ideal($\bar{b} = 0.5$) dusty magneto-gasdynamics for $\gamma = 1.67$, $Z = 0.01$, $\beta = 0.8$, $\tilde{Y}_s''(0) = 0.7$.

The comparative study for all instances is shown in Fig.4.4 and 4.5 which indicates the formation of shock for ideal and non-ideal case by increasing the amount of dust particles and magnetic field effects together. Fig.4.4 depicts the larger value of y_r for axisymmetric case which indicates early shock formation in case of plane beak

case for ideal gas. Fig.4.5 shows delayed shock formation for axisymmetric case as compared to plane beak case for non-ideal gas.

4.6 Conclusion

In this work, we have used wavefront analysis method to study the growth and decay behavior of shock waves for planar and non-planar cases in 2-D steady supersonic dusty non-ideal inviscid flow of magnetogasdynamics. We focus on the combined effect of dust particles with magnetic field in non-ideal gas to understand the evolutionary behavior of shocks. We have described what physical changes take place when we change the values of physical parameters required for the motion. The distance at which the characteristic curves intersect is evaluated, and the conditions that ensure no shock will ever form on the wavefront is determined. It is found that the shock formation completely depends on the upstream flow Mach number M_0, the magnetic field parameter ϵ_0 and initial body curvature which may be either $\tilde{Y}_a''(0)^{-1}$ or $\tilde{Y}_s''(0)^{-1}$, non-ideal parameter $\bar{b}$ and k_p, which represents the presence of dust particles. It is observed that in the presence of dust particles with magnetic field in non-ideal gas, increases the shock formation distance y_r which indicates that there is delay in the formation of shock. Also, we depict the effects graphically for both ideal and non-ideal cases. The findings of this study for non-magnetic case, i.e., for $\epsilon = 1$, closely match with the findings of previous studies, (Chaturvedi et al. [160]). Also, for the non-magnetic case, with $\bar{b} = 0$, the results obtained in this study are comparable to those found in the literature (Chaturvedi et al. [94]).

The potential applications of shock wave in dusty gas with magnetic field are in active rocket experiments in near-Earth space and formation of transient atmospheres

of atmosphere-less cosmic bodies, due to the impacts of large meteoroids or man-made projectiles with these bodies. Also, this can be related to some questions that are studied in astrophysical plasmas. The layer of dust behind the supernova shock is observed usually. The problem is to verify whether the layer of dust is related to the process of dust condensation behind the shock wavefront. One believes that most of new stars are formed in dust-molecular clouds, and shock wave starts this process. They create an increase in density sufficiently for the gravitational self-compression. The observations show that the presence of dust is connected with star formations. In particular, there are direct observations of star formation in dusty clouds.

****